Catalysis Today 179 (2012) 78–84

Contents lists available at ScienceDirect

Catalysis Today

journal homepage: www.elsevier.com/locate/cattod

Acylation of *p*-xylene over zeolites

D. Procházková*, L. Kurfiřtová, J. Pavlatová

J. Heyrovský Institute of Physical Chemistry, Academy of Sciences of the Czech Republic, v.v.i., Prague CZ-182 23, Czech Republic

ARTICLE INFO

Article history:
Received 29 April 2011
Received in revised form 27 June 2011
Accepted 28 June 2011
Available online 28 July 2011

Keywords:
Acylation
p-Xylene
Zeolites
Structural types
Acidity

ABSTRACT

Zeolites differing in structure and acidity were tested in liquid phase acylation of *p*-xylene. Hexanoyl chloride, propionic anhydride and isobutyric anhydride were used as acylating agents. The highest conversions of acylating agent were achieved over large pore zeolites USY (66.3%) and Beta (58.2%). It was found that acylation of *p*-xylene proceeds only over large pore zeolites Beta and USY. Selectivities to monoacylated *p*-xylene obtained over USY zeolite decreased in the order: propionic anhydride 78.0% > hexanoyl chloride 67.2% > isobutyric anhydride 33.1%. Diacylated product was formed over zeolite USY with all acylating agents tested but only with hexanoyl chloride over zeolite Beta. It was found that the optimum Si/Al ratio of zeolite Beta for *p*-xylene acylation with propionic anhydride is 25, while for isobutyric anhydride is 19. Conversion of isobutyric anhydride decreased with increasing isobutyric anhydride concentration and increased with increasing amount of catalyst.

1. Introduction

Aromatic ketones are important intermediates in the synthesis of fine chemicals. Friedel–Crafts acylation is one of the typical reactions for preparing these compounds. Traditionally, the Friedel–Crafts catalysts such as $AlCl_3$, $FeCl_3$ or strong protic acids like H_2SO_4 and HF are usually used. The major drawback is that they are not regenerable and must be used in more than stoichiometric amounts. Hydrolysis of a complex between ketone and catalyst results in the formation of highly corrosive waste streams. Using heterogeneous catalysts may overcome these problems. The most frequently used heterogeneous catalysts for acylation reactions are zeolites [1–5], mesoporous molecular sieves [6–8], clays [3,9], sulfated zirconia [3,10,11], heteropolyacids [3,12,13] and Nafion [3,14]. Zeolite based catalysts are the most promising group of catalysts for acylation reactions. Acylation of anisole [15,16], veratrole [17–19], biphenyl [20,21] and toluene [8,22,23] over zeolites was widely studied and reported in the literature.

Dimethylbenzophenones are used for the production of dyes and several organic intermediates for the production of fine chemicals [24]. Acylation of *p*-xylene with benzoyl chloride over zeolite Beta was studied by Jacob et al. providing almost only monoacylated product 2,5-dimethylbenzophenone with a benzoyl chloride conversion 22.1% and a selectivity of 96.7% [24]. Chiche et al. studied acylation of *p*-xylene with octanoic acid over ion exchanged Al^{3+} montmorillonite. The yield of 1-(2,5-dimethylphenyl)octan-1-one was 50% [25]. Izumi et al. used Keggin-type heteropolyacids $K_{2.5}H_{0.5}PW_{12}O_{40}$, $Rb_{2.5}H_{0.5}PW_{12}O_{40}$, $Cs_{2.5}H_{0.5}PW_{12}O_{40}$, $Cs_{2.5}H_{0.5}PMo_{12}O_{40}$, $K_2H_2SiW_{12}O_{40}$, $Cs_2H_2SiW_{12}O_{40}$ and $(NH_4)_2HPW_{12}O_{40}$ besides the zeolite catalysts in *p*-xylene acylation with benzoyl chloride. The conversions of benzoyl chloride achieved over heteropolyacid catalysts (77–39%) were higher than that obtained over zeolites HY and LaY (9%) [26]. Yield of 2,5-dimethylbenzophenone was 74%. Pure phosphotungstic acid ($H_3PW_{12}O_{40}$) supported on SiO_2 in the Cs form was studied in the acylation of *p*-xylene with crotonic acid [27]. The ketone product formed by direct acylation by crotonic acid was not found in the reaction mixture. Major reaction pathway was the acylation of *p*-xylene followed by intramolecular alkylation by the double bond affording indanone as the main reaction product [27]. Choudhary et al. observed yield of 2,5-dimethylbenzophenone 74% in acylation of *p*-xylene with benzoyl chloride over $InCl_3$ impregnated MCM-41 [28]. The moisture insensitivity of the catalyst indicated that acylation reaction was not catalyzed by Lewis acid sites and the high acylation activity was attributed to redox property of $InCl_3$/MCM-41. Deutsch et al. studied acylation of *p*-xylene with benzoic anhydride over sulfated zirconia ZrO_2/SO_4. The yield of 2,5-dimethylbenzophenone was 82% [29].

This contribution is aimed at studying the acylation of *p*-xylene with acid anhydrides and acyl chlorides over different structural types of zeolites. The effect of the catalyst structure, its acidity and type of acylating agent on the conversion and selectivity in *p*-xylene acylation was tested. In addition, the various factors such as the effect of the amount of the catalyst, the molar ratio acylating agent/substrate on the course of the reaction were investigated.

* Corresponding author.
E-mail address: dana.prochazkova@jh-inst.cas.cz (D. Procházková).

0920-5861/$ – see front matter © 2011 Elsevier B.V. All rights reserved.
doi:10.1016/j.cattod.2011.06.033

Table 1
Characteristics of zeolites used.

Zeolite	Origin	Channel structure	Channel entrances	Channel diameter (nm)	c_{LC} (mmol/g)	c_{BC} (mmol/g)	Si/Al ratio
Beta	Zeolyst	3D	12-12-12	0.64 × 0.76 0.56 × 0.56	0.45	0.14	12.5
					0.18	0.28	19.0
					0.19	0.33	25.0
					0.07	0.08	75.0
					0.03	0.05	150.0
USY	Zeolyst	3D	12	0.74	0.34	0.20	15.0
MOR	Zeolyst	2D	12-8	0.65 × 0.70 0.26 × 0.57	0.35	0.56	10.0
ZSM-5	Conteca	3D	10-10-10	0.53 × 0.56 0.51 × 0.55	0.20	0.73	11.5
FER	Zeolyst	2D	10-8	0.42 × 0.54 0.35 × 0.48	0.06	0.44	27.5

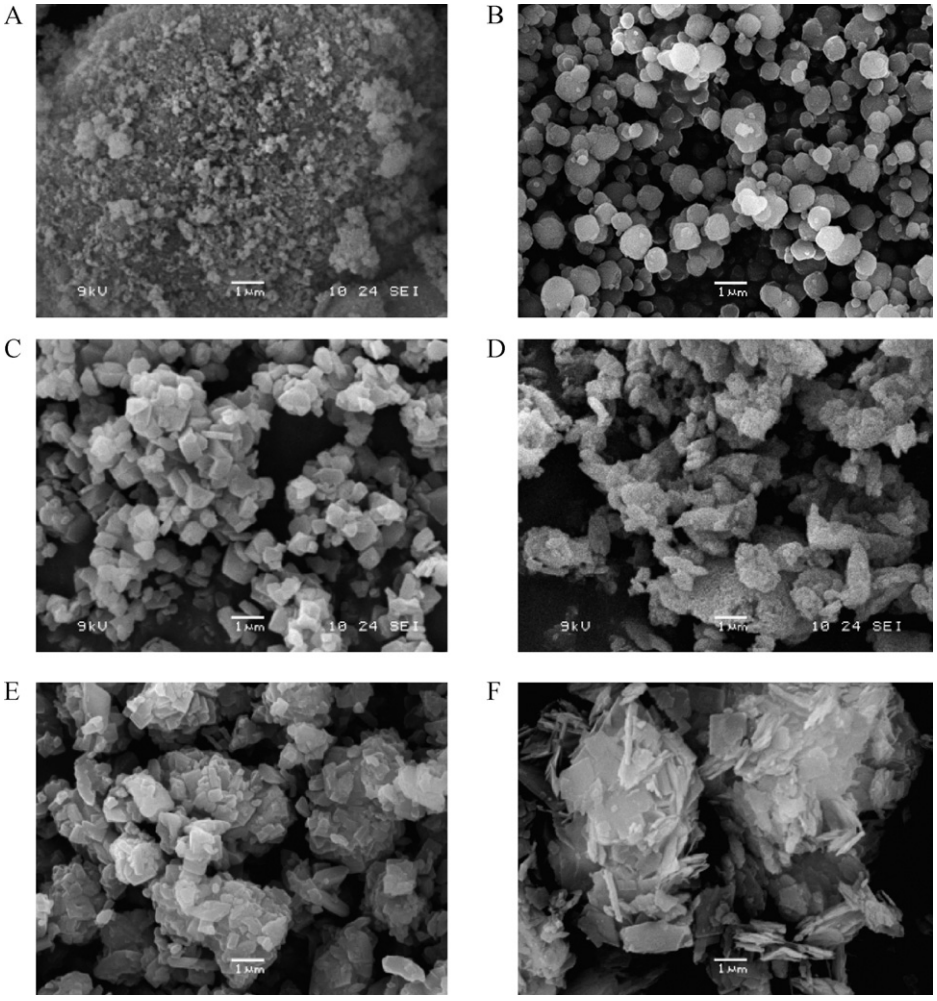

Fig. 1. SEM images of zeolite Beta/12.5 (A), Beta/19 (B), USY (C), mordenite (D), ZSM-5 (E), and ferrierite (F).

2. Experimental

2.1. Chemicals and catalysts

All chemicals used were purchased from Sigma Aldrich. Hexanoyl chloride, propionic anhydride and isobutyric anhydride were used as acylating agents, *p*-xylene as substrate and zeolites differing in their structure and acidity were used as catalysts.

2.2. Characterization

Different structural types of zeolites with different Si/Al ratios were used in acylation of *p*-xylene (Beta, USY, ZSM-5, mordenite and ferrierite). All zeolite catalysts used in catalytic tests were in H-form. Characteristics of zeolites used are given in Table 1.

The crystallinity of zeolites was determined by X-ray powder diffraction with Bruker D8 X-ray powder diffractometer using CuKα radiation in the Bragg-Brentano geometry.

X-ray diffraction patterns of all zeolites provided clear evidence of high crystallinity and phase purity of samples under investigation.

The concentration of Lewis and Brønsted acid sites was determined by adsorption of d_3-acetonitrile as a probe molecule followed by FTIR spectroscopy (Nicolet 6700) using self-supported wafer technique. A thin zeolite wafer was activated prior to the experiment in a high vacuum (10^{-4} Torr) at the temperature of 450 °C overnight. Adsorption of d_3-acetonitrile proceeded at room temperature for 30 min at a partial pressure of 5 Torr and was followed by 20 min evacuation. The molar absorption coefficients for d_3-acetonitrile adsorbed on Brønsted acid sites

(ν(C≡N)-B at 2297 cm^{-1}, ε(B) = 2.05 ± 0.1 cm μmol^{-1}) and strong and weak Lewis acid sites (ν(C≡N)-L_1 at 2325 cm^{-1} and ν(CN)-L_2 at 2310 cm^{-1}, ε(L) = 3.6 ± 0.2 cm μmol^{-1}) were used to obtain quantitative analysis of Brønsted and Lewis acid sites [30].

The size and shape of zeolite crystals were determined by scanning electron microscopy using an instrument Jeol, JSM-5500LV.

2.3. Catalytic tests

Acylation of *p*-xylene was carried out in a liquid phase under atmospheric pressure at reaction temperature of 130 °C in a multi-experiment work station StarFish (Radleys Discovery Technologies, UK). The reactions were performed in a 50 mL round bottom flask equipped with a condenser. In a typical experiment, 97 mmol of substrate, 16 mmol of acid anhydride or acyl chloride, 0.5 g of dodecane (internal standard) and 1 g of catalyst were used. The catalysts were activated prior to the catalytic experiment by heating at 450 °C for 90 min with a temperature rate 10 °C/min and then cooled in a dessicator. Catalytic test was carried out as follows: activated catalyst, internal standard, substrate were introduced in the flask, stirred and heated. Acylating agent was added into the vessel through a syringe when the desired reaction temperature was reached. Samples of the reaction mixture were taken periodically from the reaction vessel and were analyzed by a gas chromatography (Agilent 6850) using nonpolar DB-5 column (length 20 m, diameter 0.18 mm, film thickness 0.18 μm). Reaction products were identified using a mass spectrometry (ThermoFinnigan, FOCUS DSQ II Single Quadrupole GC/MS).

3. Results and discussion

3.1. Catalyst characterization

X-ray powder patterns of all commercial zeolites used in this work exhibited a high crystallinity and phase purity (not shown in this paper).

Fig. 1 provides SEM images of zeolites used. Commercial zeolites Beta/12.5 (A) and Beta/75 exhibit small particles size about 0.1 μm in diameter, while zeolite Beta/25 has particle size about 0.3 μm, Beta/150 0.5 μm and Beta/19 (B) about 0.8 μm. Zeolite USY (C) exhibits particle size about 1 μm, mordenite (D) about 1.5 μm, ZSM-5 (E) 1.5 μm and ferrierite (F) has particles size about 2 μm (Fig. 1).

Morphology of tested zeolites is considerably different. Zeolite Beta/19 exhibits uniform round shape crystals while crystals of zeolite Beta/12.5 and USY are not evenly shaped. Ferrierite, mordenite and ZSM-5 form small aggregates composed of irregularly shaped particles.

The concentration of acid sites in zeolites studied was determined by FTIR spectroscopy.

Fig. 2 provides characteristic FTIR spectra of zeolites Beta, USY, mordenite, ZSM-5 and ferrierite, in the region of hydroxyl groups and those after adsorption of d_3-acetonitrile giving rise to the absorption bands of d_3-acetonitrile interacting with Lewis and Brønsted acid sites. The band observed at 3745 cm^{-1} can be assigned to terminal silanol groups. For zeolite USY, two hydroxyl groups are observed at 3565 cm^{-1} and 3630 cm^{-1}, attributed to protons in 6-ring windows of the sodalite cages and pointing into supercages [31]. The IR spectra of the OH stretching region for zeolites ZSM-5, Beta and mordenite possess band at 3610 cm^{-1} being characteristic of acidic bridging hydroxyl groups. In the case of ferrierite, the band characteristic of Brønsted acid sites is visible at 3600 cm^{-1} [32]. Adsorption of d_3-acetonitrile removed these bands while new bands in the region 2350–2250 cm^{-1} appeared. Band at 2325 cm^{-1} is attributed to the adsorption of d_3-acetonitrile on

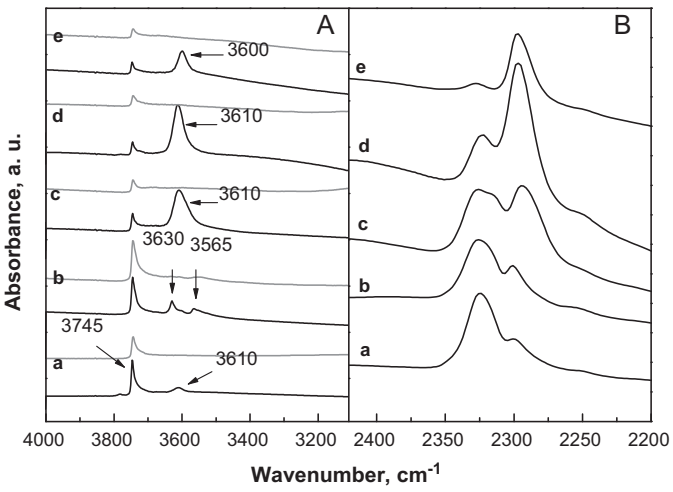

Fig. 2. IR spectra of hydroxyl vibration region (A) and spectra of d_3-acetonitrile region after its adsorption (B) of zeolite Beta/12.5 (a), USY (b), mordenite (c), ZSM-5 (d) and ferrierite (e) for (A) black line: spectra of activated samples, grey line: spectra after 20 min desorption at room temperature.

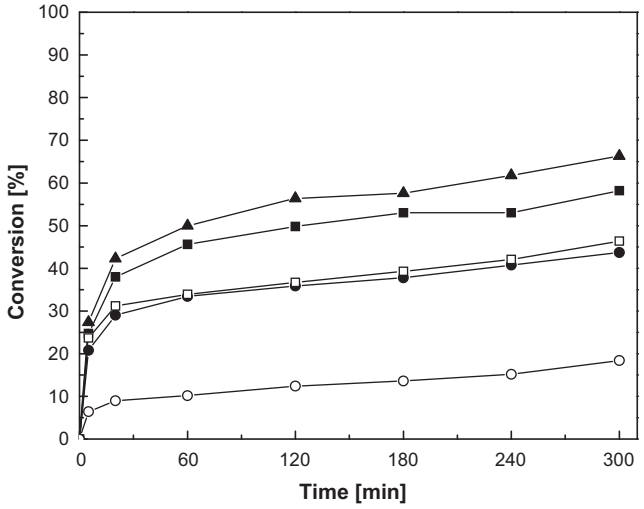

Fig. 3. Conversion of hexanoyl chloride in acylation of *p*-xylene, (■) Beta/12.5, (▲) USY/15, (●) ZSM-5, (□) mordenite, and (○) ferrierite (1 g cat., 130 °C).

Lewis acid sites and absorption band at 2300 cm^{-1} indicates the H-bond between d_3-acetonitrile and the acid OH groups in the zeolite [33].

3.2. The effect of the structure of the catalyst

Zeolites differing in dimensionality, connectivity of the channels and pore sizes were studied in *p*-xylene acylation in order to investigate differences in their catalytic behavior. Hexanoyl chloride, propionic anhydride and isobutyric anhydride were used as acylating agents.

The highest hexanoyl chloride conversions were achieved over zeolite USY 66.3% and Beta 58.2% (1 g cat., 130 °C, 300 min of the reaction, Fig. 3). This can be attributed to their three-dimensional large pore channel structure. Moreover, pores of USY zeolite should allow readier diffusion than those of the Beta zeolite. Conversions of hexanoyl chloride obtained over zeolites Beta and USY were similar in spite of the fact that crystal size of zeolite Beta is 0.1 μm and USY 1 μm. It is seen that the structure and dimensionality of zeolite is prevailing the size of the crystals in *p*-xylene acylation. The lowest conversion of hexanoyl chloride was obtained over ferrierite

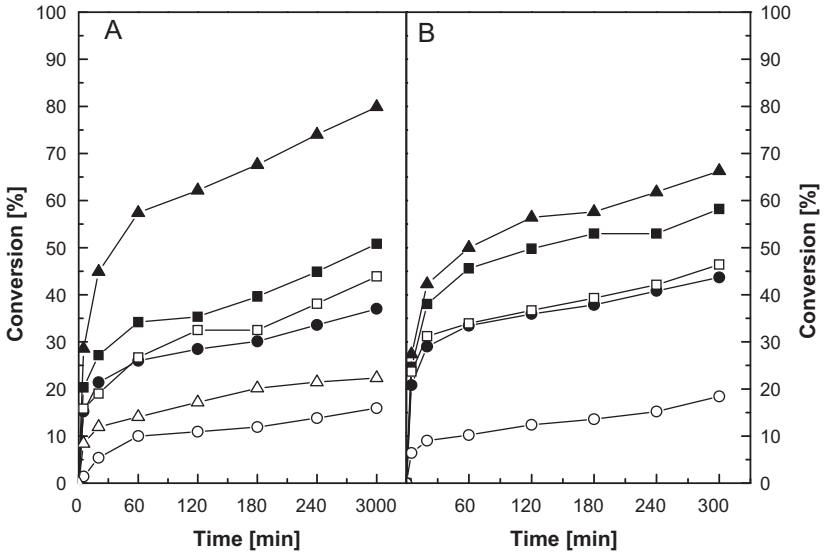

Fig. 4. Acylation of *p*-xylene with (A) propionic anhydride and (B) isobutyric anhydride, (■) Beta/12.5, (●) USY/15, (▲) ZSM-5, (□) mordenite, and (○) ferrierite.

18.4% probably due to small size of the channels and large crystal size about 2 μm. In addition, a decrease in hexanoyl chloride conversions corresponds also to the decrease in the concentration of Lewis acid sites of tested zeolites. It is known that both types of zeolite acid centers participate in the acylation reaction. Ma et al. [34] studied acylation of anisole with propionic acid and described that propionic acid is either protonated by Brønsted acid sites or coordinated on Lewis acid sites of the zeolite. The coordinated form is more reactive for the attack the aromatic ring than the protonated form. It is assumed that adsorption of acylating agent onto Brønsted acid site is stronger than the adsorption onto Lewis acid site resulting from coordination character of the bond. Moreover, strong adsorption of the reactants on acid sites could limit the access of other reactants, which can cause diffusion limitation problems [34].

Sequence of conversions of propionic anhydride was as follows: Beta 51.1% > USY 44.2% > mordenite 38% > ZSM-5 37.3% > ferrierite 11.7% (Fig. 4A).

The highest propionic anhydride conversions were obtained over three-dimensional large pore zeolites as in the case of hexanoyl chloride.

On the contrary, higher propionic anhydride conversion was achieved over zeolite Beta than over USY. The main reason is probably that the difference in the hydrophilicity of these zeolites leading to differences in the adsorption of different acylating agents used and following differences in conversions [16]. The lowest conversion of propionic anhydride was obtained over ferrierite combining 10- and 8-ring channels. It can be indicated that all active centers are not accessible for the reactants and that the reaction proceeds mainly on the external surface of ferrierite.

Finally, isobutyric anhydride conversions as well as increased from 10-membered zeolites to 12-membered zeolites. The highest conversion of isobutyric anhydride was obtained over USY zeolite 52.7% (Fig. 4B). The size of the crystals of mordenite, ZSM-5 and USY is almost the same about 1 μm. Difference in conversions of isobutyric anhydride over mordenite and ZSM-5 was 0.4% (achieved conversions were 43.7 and 44.1%, respectively) while isobutyric anhydride conversion reached over zeolite USY was 52.7%. It indicates that transport of reactants and products in porous system of mordenite and ZSM-5 is rather limited due to small channels and that the reaction proceeds mainly on the external surface.

Conversions of acylating agent over zeolite USY decreased in the order: hexanoyl chloride 66.3% > isobutyric anhydride 52.7% > propionic anhydride 44.2%. The acid chlorides are usually more reactive than acid anhydrides [35]. Conversions of isobutyric anhydride were higher than propionic anhydride conversions in spite of the fact that steric constraints of isobutyric anhydride and corresponding products are higher than of propionic anhydride. Higher activity of propionic anhydride in comparison with acetic anhydride was observed by Chidambaram in biphenyl acylation [20].

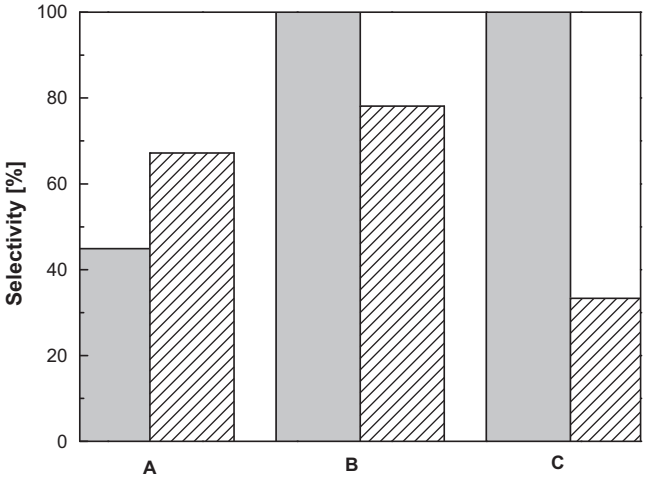

Fig. 5. Selectivity to (A) 1-(2,5-dimethylphenyl)hexan-1-one, (B) 1-(2,5-dimethylphenyl)propan-1-one and (C) 1-(2,5-dimethylphenyl)-2-methylpropan-1-one in *p*-xylene acylation with hexanoyl chloride (A), propionic (B) and isobutyric (C) anhydride over ▩ Beta and ▨ USY at conversion of acylating agent equal to 40%.

Selectivity to particular ketone product in acylation of *p*-xylene is influenced by the different structure architecture of catalyst used (Fig. 5). Acylation of *p*-xylene led to monoacylated *p*-xylene (1-(2,5-dimethylphenyl)hexan-1-one (Fig. 6A), 1-(2,5-dimethylphenyl)propan-1-one (Fig. 6B) and 1-(2,5-dimethylphenyl)-2-methylpropan-1-one (Fig. 6C)), as the main reaction product only over zeolites Beta and USY.

In the case of acid anhydrides selectivities to monoacylated product over zeolite Beta (100%) were higher than selectivities obtained over zeolite USY, while selectivity to monoacylated *p*-xylene was higher over USY than over Beta with hexanoyl

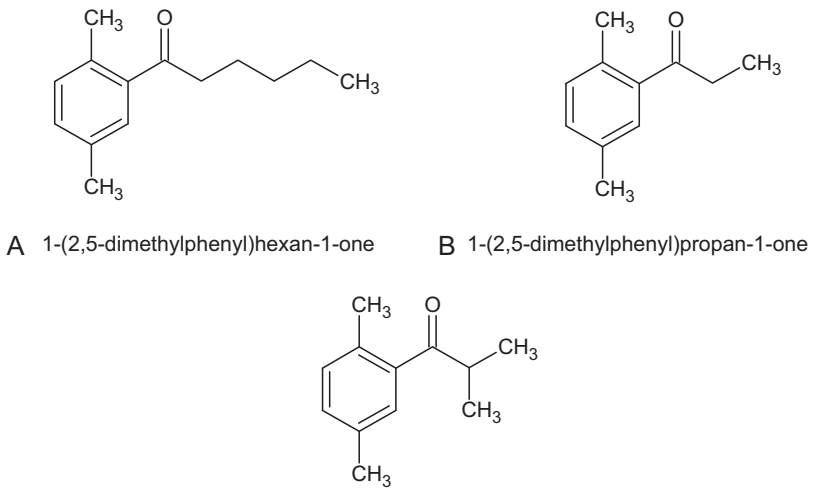

Fig. 6. Products formed in *p*-xylene acylation with hexanoyl chloride (A), propionic anhydride (B) and isobutyric anhydride (C).

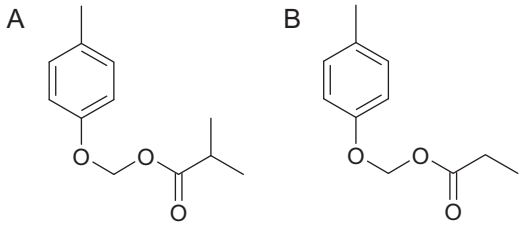

Fig. 7. The reaction product in acylation of *p*-xylene with isobutyric anhydride. (A) (4-methylphenoxy)methyl-2-methylpropanoate and propionic anhydride and (B) (4-methylphenoxy)methyl propanoate.

chloride. Selectivities to monoacylated *p*-xylene over USY zeolite were following: propionic anhydride 78.0% > hexanoyl chloride 67.2% > isobutyric anhydride 33.1% (conversion of acylating agent 40%). Strong adsorption of the reactants on acid sites could limit the access of other reactants, which can cause diffusion limitation problems.

Diacylated *p*-xylene was formed over zeolite USY with hexanoyl chloride 1.7%, isobutyric anhydride 56.4% and propionic anhydride 21.9% (conversion of acylating agent 40%). The *p*-xylene acylation to the second level is probably enabled by the presence of large cavities in the structure of USY zeolite. *p*-Xylene acylation over zeolite Beta resulted in diacylated product only with hexanoyl chloride 1.9% (conversion of acylating agent 40%). Formation of diacylated product with selectivity up to 2% was suppressed by steric hindrances of the bulky molecule in *p*-xylene acylation with hexanoyl chloride.

Acylation of *p*-xylene did not proceed over zeolites ZSM-5, mordenite and ferrierite with all acylating agents used. Acylated *p*-xylene is not formed probably due to geometrical constraints induced by small channels of ZSM-5, mordenite and ferrierite.

In this case parallel reaction of hexanoyl chloride leading to hexanoic anhydride occurred. The reason probably is that due to presence of small amount of water retained in the zeolite pores hydrolysis of hexanoyl chloride took place and that the hexanoic acid reacted afterwards with hexanoyl chloride forming hexanoic anhydride.

In the case of acid anhydrides the main reaction product was (4-methylphenoxy)methyl-2-methylpropanoate and (4-methylphenoxy)methyl propanoate, respectively (Fig. 7). The presence of the products A and B (Fig. 7) were confirmed by GC–MS and NMR spectroscopy. Lapitskiy et al. reported that *p*-xylene oxidation in the presence of acetic anhydride and sulfuric acid as catalyst led to (4-methylphenoxy)methyl acetate [36]. A similar compound was isolated and identified in toluene oxidation. The authors suggest that reaction passes through the stage of hydroperoxides formation with subsequent rearrangement to hemiacetals. After interaction of hemiacetal with acetic anhydride (4-methylphenoxy)methyl acetate is formed.

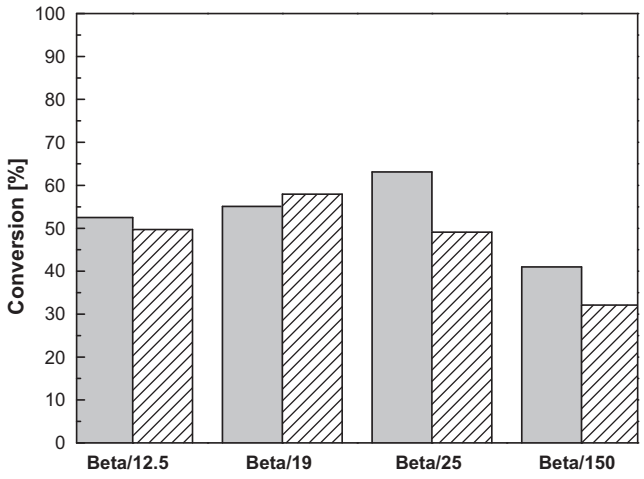

Fig. 8. The effect of the Si/Al ratio on the conversion of propionic anhydride ▭ and isobutyric anhydride ▨ in *p*-xylene acylation over zeolite Beta (1 g cat., 130 °C, 300 min of the reaction).

In the case of propionic anhydride the selectivity to (4-methylphenoxy)methyl propanoate (Fig. 7B) was 100% over ZSM-5, mordenite and ferrierite (propionic anhydride conversion 10%), while with isobutyric anhydride the selectivity to (4-methylphenoxy)methyl 2-methylpropanoate (Fig. 7A) was 57.1% over ZSM-5, 61.8% over mordenite and 61.7% over ferrierite (isobutyric anhydride conversion 10%).

3.3. The effect of the Si/Al ratio

Zeolite Beta with different Si/Al ratios was tested in *p*-xylene acylation in order to understand the effect of the acidity of zeolite to conversion of acylating agent. The conversions of propionic anhydride and isobutyric anhydride are depicted in Fig. 8.

Table 2
The effect of the amount of catalyst.

The amount of catalyst [g]	Conversion of isobutyric anhydride [%]
0.2	30.2
0.6	39.2
1	57.9
1.4	67.7
1.8	81.6

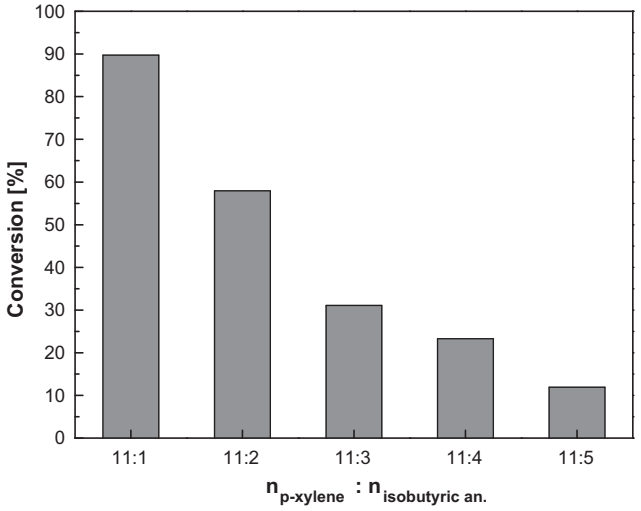

Fig. 9. The effect of the *p*-xylene/isobutyric anhydride molar ratio (1 g Beta/19, 130 °C, 300 min of the reaction).

It was found that for acylation of *p*-xylene with propionic anhydride the optimum concentration of active site contains zeolite Beta with Si/Al ratio 25 while for isobutyric anhydride the highest conversion of isobutyric anhydride was obtained over zeolite Beta with Si/Al ratio 19. This result is in good agreement with literature. Červený et al. reported that in naphthalene acylation, the highest conversion of naphthalene was achieved over zeolite Beta with Si/Al 37.5 [37]. Naphthalene conversion over zeolites possessing a higher concentration of active sites was lower due to rapid deactivation of catalyst. The lowest naphthalene conversion was obtained over zeolite Beta with the lowest concentration of active sites [38]. Such a behavior was confirmed in acylation of cyclohexene with propionic anhydride over zeolite Beta [33].

In acylation of anisole with phenylacetyl chloride over dealuminated Y zeolites yield of acylated product increased with increasing Si/Al ratio probably due to increasing hydrophobicity of the zeolites [15]. Wagholikar et al. obtained the same results in acylation of anisole over zeolites Y, Beta and mordenite. They explained this behavior by the creation of mesopores in the dealuminated samples and easier diffusion of the reactants and products [16]. But in ferrocene acylation with cinnamoyl chloride and adamantoyl chloride and in *o*-xylene acylation with benzoyl chloride over Beta zeolite the conversion decreased with increasing Si/Al ratio probably due to different hydrophobicity of ferrocene in comparison with other aromatic compounds [24,39].

3.4. The effect of the ratio substrate/acylating agent

Acylation of *p*-xylene with isobutyric anhydride over Beta/19 was investigated with different molar ratios of *p*-xylene/acylating agent. It is clearly seen that with increasing concentration of acylating agent conversion of isobutyric anhydride decreases (Fig. 9). The reason could be that adsorption/desorption equilibrium is shifted to reactants with increasing amount of acylating agent as was reported in acylation of toluene [23,40]. The excess of acylating agent increases the concentration of acylium ions which can probably block the entrance of zeolite pores. Jaimol et al. [41] observed decreasing conversion of veratrole with increasing concentration of acylating agent in acylation of veratrole with propionyl chloride. Increase in benzoyl chloride conversion with increasing *o*-xylene/benzoyl chloride molar ratio was reported as well as by Jacob et al. [24].

3.5. The effect of the amount of the catalyst

The effect of the different amount of catalyst on isobutyric anhydride conversion is depicted in Table 2 (Beta/19, 130 °C, 300 min). The increase in the conversion of isobutyric anhydride with increasing amount of the zeolite catalyst was attributed to the proportional increase in the number of active sites.

4. Conclusions

Acylation of *p*-xylene was investigated over different structural types of zeolites differing in Si/Al ratio with hexanoyl chloride, propionic anhydride and isobutyric anhydride. The highest conversions of acylating agent were achieved over large pore zeolites Beta and USY. Conversions of acylating agent over zeolite USY decreased in the order: hexanoyl chloride 66.3% > isobutyric anhydride 52.7% > propionic anhydride 44.2%. Monoacylated *p*-xylene was formed over zeolites USY and Beta. Selectivities to monoacylated *p*-xylene achieved over zeolite USY were as follows: propionic anhydride 78.0% > hexanoyl chloride 67.2% > isobutyric anhydride 33.1% (conversion of acylating agent 40%). In the case of acylation of *p*-xylene over zeolites ZSM-5, mordenite and ferrierite with hexanoyl chloride, the main reaction product was hexanoic anhydride. Reaction of *p*-xylene with propionic anhydride and isobutyric anhydride led to (4-methylphenoxy)methyl propanoate and (4-methylphenoxy)methyl 2-methylpropanoate, respectively. It was found that there is an optimal Si/Al ratio of zeolite Beta for *p*-xylene acylation with propionic anhydride Si/Al 25 and with isobutyric anhydride Si/Al 19.

It was also observed that the conversion of isobutyric anhydride decreased with increasing concentration of isobutyric anhydride and increased with increasing amount of the catalyst.

Acknowledgements

The authors thank the Grant Agency of the Czech Republic for financial support (104/07/0383, 203/08/H032).

References

[1] M.L. Kantam, K.V. Ranganath, M. Sateesh, K.B.S. Kumar, B.M. Choudary, J. Mol. Catal. A: Chem. 225 (2005) 15–20.
[2] M. Bejblová, D. Procházková, J. Čejka, ChemSusChem 2 (2009) 486–499.
[3] G. Sartori, R. Maggi, Chem. Rev. 106 (2006) 1077–1104.
[4] C.P. Bezouhanova, Appl. Catal. A 229 (2002) 127–133.
[5] H. van Bekkum, A.J. Hoefnagel, M.A. van Koten, E.A. Gunnewegh, A.H.G. Vogt, H.W. Kouwenhoven, Stud. Surf. Sci. Catal. 83 (1994) 379–390.
[6] Z. El Berrichi, L. Cherif, O. Orsen, J. Fraissard, J.P. Tessonnier, E. Vanhaecke, B. Louis, M.J. Ledoux, C. Pham-Huu, Appl. Catal. A 298 (2006) 194–202.
[7] D. Procházková, M. Bejblová, J. Vlk, A. Vinu, P. Štěpnička, J. Čejka, Chem. Eur. J. 16 (2010) 7773–7780.
[8] A. Vinu, T. Krithiga, N. Gokulakrishnan, P. Srinivasu, S. Anandan, K. Ariga, V. Murugesan, V.V. Balasubramanian, T. Mori, Micropor. Mesopor. Mater. 100 (2007) 87–94.
[9] V.R. Choudhary, S.K. Jana, J. Catal. 201 (2001) 225–235.
[10] J. Deutsch, A. Trunschke, D. Muller, V. Quaschning, E. Kemnitz, H. Lieske, J. Mol. Catal. A: Chem. 207 (2004) 51–57.
[11] V. Quaschning, J. Deutsch, P. Druska, H.J. Niclas, E. Kemnitz, J. Catal. 177 (1998) 164–174.
[12] J. Kaur, K. Griffin, B. Harrison, I.V. Kozhevnikov, J. Catal. 208 (2002) 448–455.
[13] I.V. Kozhevnikov, Appl. Catal. A 256 (2003) 3–18.
[14] A. Heidekum, M.A. Harmer, W.F. Hölderich, J. Catal. 188 (1999) 230–232.

[15] A. Corma, M.J. Climent, H. Garcia, J. Primo, Appl. Catal. 49 (1989) 109–123.
[16] S.G. Wagholikar, P.S. Niphadkar, S. Mayadevi, S. Sivasanker, Appl. Catal. A 317 (2007) 250–257.
[17] V.V. Balasubramanian, P. Srinivasu, C. Anand, R.R. Pal, K. Ariga, S. Velmathi, S. Alam, A. Vinu, Micropor. Mesopor. Mater. 114 (2008) 303–311.
[18] A. Vinu, Adv. Funct. Mater. 18 (2008) 816–827.
[19] A. Vinu, J. Justus, C. Anand, D.P. Sawant, K. Ariga, T. Mori, P. Srinivasu, V.V. Balasubramanian, S. Velmathi, S. Alam, Micropor. Mesopor. Mater. 116 (2008) 108–115.
[20] M. Chidambaram, C. Venkatesan, P. Moreaub, A. Finiels, A.V. Ramaswamy, A.P. Singh, Appl. Catal. A 224 (2002) 129–140.
[21] J.M. Escola, M.E. Davis, Appl. Catal. A 214 (2001) 111–120.
[22] M. Bejblová, D. Procházková, J. Vlk, Top. Catal. 52 (2009) 178–184.
[23] J. Klisáková, L. Červený, J. Čejka, Appl. Catal. A 272 (2004) 79–86.
[24] B. Jacob, S. Sugunan, A.P. Singh, J. Mol. Catal. A: Chem. 139 (1999) 43–53.
[25] B. Chiche, A. Finiels, C. Gauthier, P. Geneste, Appl. Catal. 30 (1987) 365–369.
[26] Y. Izumi, M. Ogawa, K. Urabe, Appl. Catal. A 132 (1995) 127–140.
[27] C. De Castro, J. Primo, A. Corma, J. Mol. Catal. A: Chem. 134 (1998) 215–222.
[28] V.R. Choudhary, S.K. Jana, N.S. Patil, Tetrahedron Lett. 43 (2002) 1105–1107.
[29] J. Deutsch, V. Quaschning, E. Kemnitz, A. Auroux, H. Ehwald, H. Lieske, Top. Catal. 13 (2000) 281–285.
[30] B. Gil, G. Košová, J. Čejka, Micropor. Mesopor. Mater. 129 (2010) 256–266.
[31] J.A. Lercher, A. Jentys, Stud. Surf. Sci. Catal. 168 (2007) 435–476.
[32] S. Kotrel, J.H. Lunsford, H. Knozinger, J. Phys. Chem. B 105 (2001) 3917–3921.
[33] M. Bejblová, J. Vlk, D. Procházková, H. Šiklová, J. Čejka, Collect. Czech. Chem. Commun. 72 (2007) 728–746.
[34] Y.D. Ma, Q.L. Wang, X.D. Ji, C.M. Zhong, Q. Qiu, Chin. Chem. Lett. 7 (1996) 233–236.
[35] B. Yuan, Z. Li, Y. Liu, S. Zhang, J. Mol. Catal. A: Chem. 280 (2008) 210–218.
[36] Y.A. Lapitskiy, M.M. Grozhan, V.V. Kamzolkin, A.N. Baskhkirov, Dokl. Chem. 205 (1972) 1107–1110.
[37] L. Červený, K. Mikulcová, J. Čejka, Appl. Catal. A 223 (2002) 65–72.
[38] D. Procházková, M. Bejblová, J. Vlk, J. Čejka, Top. Catal. 52 (2009) 618–626.
[39] M. Bejblová-Voláková, J. Vlk, D. Procházková, Top. Catal. 53 (2010) 1411–1418.
[40] P. Botella, A. Corma, J.M. Lopez-Nieto, S. Valencia, R. Jacquot, J. Catal. 195 (2000) 161–168.
[41] T. Jaimol, P. Moreau, A. Finiels, A.V. Ramaswamy, A.P. Singh, Appl. Catal. A 214 (2001) 1–10.